Available online at www.sciencedirect.com
SCIENCE DIRECT
Journal of Photochemistry and Photobiology A: Chemistry 179 (2006) 130–134
Journal of Photochemistry and Photobiology A:Chemistry
www.elsevier.com/locate/jphotochem

The use of binary TiO_2–GeO_2 oxide electrodes to enhanced efficiency of dye-sensitized solar cells

Athapol Kitiyanan, Taku Kato, Yoshikazu Suzuki, Susumu Yoshikawa *

Institute of Advanced Energy, Kyoto University, Uji, Kyoto 611-0011, Japan

Received 4 May 2005; received in revised form 29 June 2005; accepted 2 August 2005
Available online 6 September 2005

Abstract

The preparation of titania (TiO_2), germania (GeO_2) and binary TiO_2–GeO_2 oxide with different Ti/Ge ratio gels based on sol–gel method with surfactant-assisted mechanism and their application for dye-sensitized solar cells (DSCs) were reported. The samples were calcined and characterized by nitrogen adsorption porosimetry, X-ray diffraction (XRD) and morphology was investigated by field emission scanning electron microscopy (FE-SEM). The XRD results suggested that germanium substituted for titanium in the TiO_2 lattice because of the gradual shift of 1 0 1 diffraction peak of anatase type of TiO_2. The higher surface area from binary oxides samples was due to the added oxide acting as a crystal growth inhibiter. For the application for DSCs, the electrodes fabricated from binary oxides sample gave significant higher J_{sc} when compared to cell that fabricated by sample TiO_2 electrode. The consequence effects of added germanium were analyzed and discussed.

Keywords: Dye-sensitized solar cell; Photoelectrochemical; Surfactant-assisted method; Titanium oxide; Germanium oxide

1. Introduction

Mesoporous film-based dye-sensitized solar cells (DSCs) have been developed since a light-activation mechanism similar to the plant photosynthetic process was applied to solar cells [1]. Typical DSC is composed of a few micrometer thick film consisting nanocrystalline oxide covered with monolayer of Ru-bipyridyl-based charge transfer dye, a redox electrolyte and a platinum metal electrode [2].

TiO_2 is well-known semiconductor oxide with band gap energy of 3.0–3.2 eV regardless of its tetragonal structure for both anatase and rutile. It is also well-known that band gap illumination generates electron–hole pairs in TiO_2. These electron–hole pairs can either recombine or move to the surface to react with species adsorbed on the surface, which is known to be the basis of photocatalysis [3], dye-sensitized solar cells is the well-known application of TiO_2 thin films. The DSCs which based on highly porous nanocrystalline films of TiO_2 are considerable attractive because of their rather high power conversion efficiency (10%), potential low cost and high semiconductor stability [4].

Although dye-sensitization can be achieved with porous films of non-TiO_2 semiconductors with high band gap such as SnO_2 [5], Fe_2O_3 [6], ZrO_2 [7], Al_2O_3 [8], ZnO [9], it has never been reported to be as efficient as the TiO_2 cells reported by O'Regan and Grätzel [10]. In fact, nanostructured TiO_2 is not perfect yet in that electron transport becomes more difficult with the increase of photocurrent in the absence of space charge layer [3]. The efficiency of DSCs is limited in part by back-reaction of photoinjected electrons with triiodide ions in the electrolyte [11] and the presences of electron acceptors such as oxygen and iodine will lead to loss of photogenerated electrons over the nanostructured semiconductor electrolyte interface during the transport of the charge transport of the electrons to the back contact [12]. Thus, photogenerated charge recombination should be prevented for enhanced efficiency because solely enlarging the oxide electrode surface area is not sufficient. In this study, germanium oxide was added to enhance the properties of TiO_2 nanostructured and would be an alternative approach to improve the photovoltaic efficiency.

* Corresponding author. Tel.: +81 774 38 3502; fax: +81 774 38 3508.
E-mail address: s-yoshi@iae.kyoto-u.ac.jp (S. Yoshikawa).

1010-6030/$ – see front matter © 2005 Elsevier B.V. All rights reserved.
doi:10.1016/j.jphotochem.2005.08.002

2. Experimental

2.1. Synthesis of pure TiO_2, pure GeO_2 and binary TiO_2–GeO_2 oxides

Preparation processes of binary TiO_2–GeO_2 oxide solid solution in this study are as follows. At first, the titania (tetra-isopropyl-orthotitanate, TIPT) and germania precursor (germanium ^{n}butoxide, GeBt) were mixed together by various concentration. The mixed metal precursors were firstly modified by modifying agent (acetylacetone, ACA) in order to obtain controllable sol–gel process. The ACA was slowly added to mixed metal precursor in a molar ratio [ACA] = 1:1 to get clear yellow mixture. The organic surfactant (laurylamine hydrochloride, LAHC) was used as micellar assemblies template structure to fabricate the well-defined mixed oxide nanocrystalline. The 0.1 M homogeneous LAHC solutions (pH 4–4.5) were mixed with the modified precursors in a molar ratio of [TIPT + GeBt]:[LAHC] = 4:1. After additions were completed, these mixtures were stirred at room temperature for 1 h and further in an oven at 40 °C for 24 h until a clear yellow solution was obtained. The reaction bottles were then sealed and kept in an oven preheated at 80 °C for 7 days to yield a gel. These gel samples were washed by iso-propanol to remove the surfactant template. All syntheses were performed in a similar step to obtain the sample which have 0, 5, 10, 20, 30 and 100 mol% of germania added (named hereafter TiGe*X*, where *X* is the mol% of germania added into titania (e.g. TiGr10 is 10 mol% of GeO_2 mixed with 90 mol% of TiO_2)). For the pure component, 'pure TiO_2' and 'pure GeO_2' will be used instead of TiGe0 and TiGe100, respectively.

2.2. Preparation of photoelectrodes

Conducting glass plates with fluorine doped tin oxide (FTO), sheet resistance 15 Ω/□ were cleaned with acetone, rinsed with distilled water and dried in 80 °C oven. The photoelectrode was prepared by doctor blade coating. As for the preparation of the starting coating gel, two longer rims of conduction glass plate (2 cm × 10 cm) were covered with adhesive tape (Scotch, ∼40 μm in thickness). Some drops of synthesized gel were applied to one of the bare edges of the conducting glass, and used a glass rod sliding over the tape-covered edges to spread the gel out evenly. The thickness of the film can be adjusted by repetitive coating and sintering at 450 °C 10 min for each layer until obtained the desire thickness. Finally, the coated electrodes were sintered at 450 °C for 2 h before measuring film thickness and fabricating DSCs.

2.3. Fabrication of dye-sensitized solar cells

After sintered in air at 450 °C for 2 h and left to be cooled to 80 °C, the sintered electrodes were then immersed in 50 wt.% butanol and 50 wt.% acetonitrile mixed solution of 0.3 mM [bis(tetrabutylammonium) cis di(thiocyanato) bis(2,2′-bipyridine-4,4′-carboxylic acid) ruthenium(II)] (called N719) dye at least 24 h. The dye-adsorbed electrodes were immediately assembled into thin layer, sandwich type solar cells. The counter electrodes, thin platinum layer sputtered on FTO conduction glass plates were kept in contact with these dyed electrodes. In order to prevent a direct contact between the working and the counter electrodes which result in the open-circuit voltage V_{oc} reduction to <300 mV [12], two stripes of 25 μm thick Surlyn (Dupont, Himilan 1702) were inserted as spacer between them. A drop of redox electrolyte composing of a 0.6 M dimethylpropyl-imidazolium iodide solution, a 0.1 M lithium iodide (LiI) solution, a 0.05 M iodide (I_2) solution and a 0.5 M 4-*tert*-butylpyridine in acetonitrile was introduced to the gap between the counter and working electrodes by the capillary force.

2.4. Characterization and measurement

Crystal structures of all samples were analyzed by X-ray diffraction (XRD) (RIGAKU Rint-2100) which is generating monochromated Cu Kα radiation with continuous scanning mode at the rate of 2 °/min and operating conditions of 40 kV and 40 mA. BET surface area of synthesized samples was recorded using nitrogen adsorption–desorption analysis (BELSORP 18 PLUS) with all samples degassed at 200 °C for 2 h before the actual measurements.

The film thickness of coated electrodes was determined by an Alpha-Step 200 apparatus (Tencor Instruments) and the amount of adsorbed dye concentration was measured by using the solution of 0.1 M NaOH and ethanol (1:1 in volume fraction), in which the anchored dye from dyed electrodes was desorbed. A shimadzu UV-2450 UV–vis spectrometer was exploited to record absorption spectra of the samples at room temperature. The sample morphology was observed by a field emission scanning electron microscopy (FE-SEM, JEOL JSM-6500FE).

The photovoltaic properties were measured by using a potentiostat (Bunko–Keiki Co., Ltd., Model HCSSP-25) irradiated with simulated solar light, A.M. 1.5, 100 mW/cm^2 (Bunko–Keiki Co., Ltd., Model CEP-2000).

3. Results and discussion

3.1. Characterization of binary TiO_2–GeO_2 oxide

Fig. 1 shows the results of XRD patterns of the pure TiO_2, pure GeO_2 and binary TiO_2–GeO_2 oxides at different Ti/Ge ratio after heat treatment at 500 °C. For the pure TiO_2, the peaks characteristic of the anatase phase appeared and no trace of rutile phase was detected. For pure GeO_2 sample, the XRD pattern exhibited hexagonal phase structure after heat treatment at 450 °C. For binary TiO_2–GeO_2 oxide samples, the XRD patterns from the sample TiGe5 to TiGe30 are in agreement with anatase type of TiO_2 and peaks from GeO_2

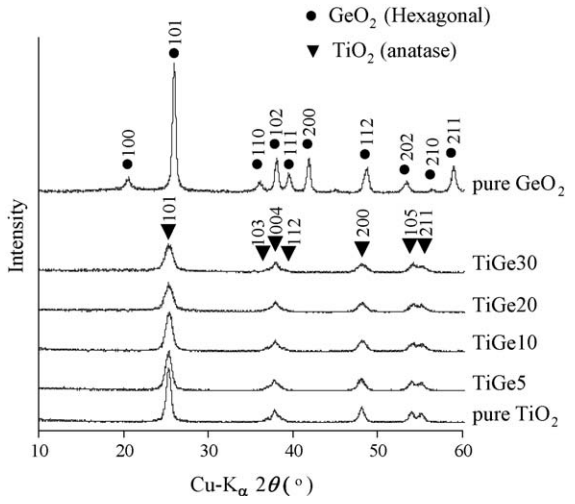

Fig. 1. XRD patterns of the pure TiO_2, GeO_2 and TiO_2–GeO_2 with different Ti/Ge ratios after heat treatment at 450 °C.

are not found in these samples. Fig. 2 shows the enlarged XRD patterns around the peak of crystal plane (1 0 1) of pure TiO_2 and binary oxide samples. The gradual shifting of the 1 0 1 diffraction peak of the anatase type titania to a higher 2θ angle with increasing germanium content suggested the substitution of titanium by germanium. It is because the ionic radius of germanium (0.53 Å) smaller than that of titanium (0.61 Å) [13]. The peaks of the sample which has germanium content >10% were not shifted probably attributed to that the germanium may not enter the TiO_2 lattice, and it may be present as GeO_2 [13]. This GeO_2 possibly presented as amorphous phase, since the XRD peaks from GeO_2 could not be observed even the germanium content reached 30 mol%.

Table 1 shows the results of BET surface area measurements. The binary TiO_2–GeO_2 oxides had much higher BET surface areas than pure TiO_2 and pure GeO_2. The increase of surface area with the amount of germanium content up to 10% was corresponding to the gradual shifting of the 1 0 1

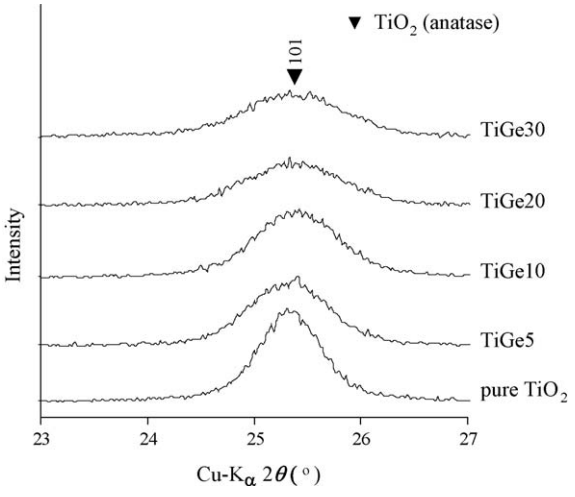

Fig. 2. Enlargement of the region around 25° 2θ of sample pure TiO_2 and mixed of different Ti/Ge ratios after heat treatment at 450 °C.

Table 1
Surface area and amount of adsorbed dyes on electrodes

Sample	BET surface area (m^2/g)	Amount of dye per thickness of the electrodes (10^{-8} mol/cm^2 μm)
Pure TiO_2	80	1.84
TiGe5	115	2.01
TiGe10	130	2.13
TiGe20	120	2.02
TiGe30	110	1.96
Pure GeO_2	22	–

diffraction peak. As the germanium atom could not enter to the lattice of TiO_2, the surface area of sample which has germanium content >10 mol% would be decrease.

3.2. Morphology of binary TiO_2–GeO_2 oxide film

Fig. 3a represents the SEM images of the surface morphology and the cross section of sample TiGe10 film with the four times repetitive coating after sintering at 450 °C for 2 h. The thicknesses of porous films are about 5 μm. This SEM image shows a fine crack-free porous electrode without a distinct cavity which can attribute to the advantages of doctor-blading method and characteristic of gel sample. The high magnification SEM images of pure TiO_2 and TiGe10 films were shown in Fig. 3b and c, respectively. The particle size distribution of pure TiO_2 is in the range of 15–30 nm and TiGe10 is 10–25 nm. The smaller in particle size of binary oxide are due to the presence of germanium as GeO_2 which inhibits crystallite growth of a solid solution [13].

3.3. Photovoltaic characteristics

Fig. 4 shows the relation of photovoltaic characteristics and oxide composition of DSCs fabricated using respective binary TiO_2–GeO_2 oxides sample: (a) short-circuit photocurrent density (J_{sc}), (b) open-circuit voltage (V_{oc}) and (c) conversion efficiency (η). Each data point was the average of five cells and the thickness of each electrode sample was controlled to be around 4 μm. J_{sc} and η were improved by increase of the amount of germanium and had a maximum at 10 mol% mixed for sample TiGe10. The change in J_{sc} is corresponding to the amount of adsorbed dye on electrode shown in Table 1. In general, the amount of adsorbed dyes increases the number of injected electrons in metal oxide electrodes, leading to an increase of J_{sc} [14,15].

Although the amount of adsorbed dye of TiGe5 and TiGe20 samples were almost the same, the J_{sc} from these two samples were significantly difference. The addition of germanium could result in changes in electrode properties depending upon the amount added. When the germanium content is <10 mol%, the added germanium could serve as a crystal growth inhibiter that can cause a higher surface area. In contrast, if the amount of added germanium is >10 mol%, a distinctive decrease in J_{sc} of the binary oxides electrodes

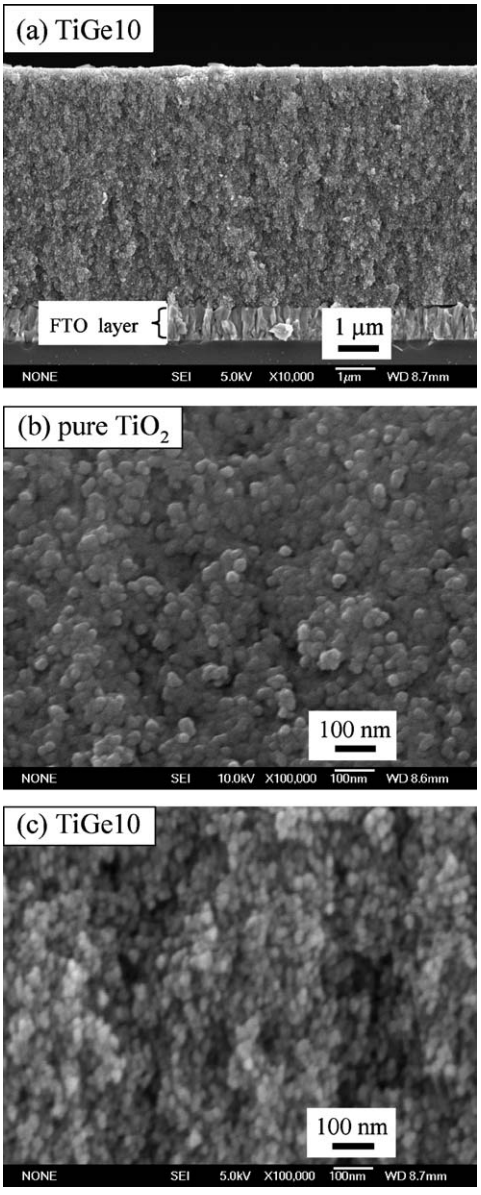

Fig. 3. FE-SEM images of (a) the cross section of sample TiGe10 electrode, (b) and (c) surface morphology of the electrode fabricated by pure TiO_2 and sample TiGe10, respectively.

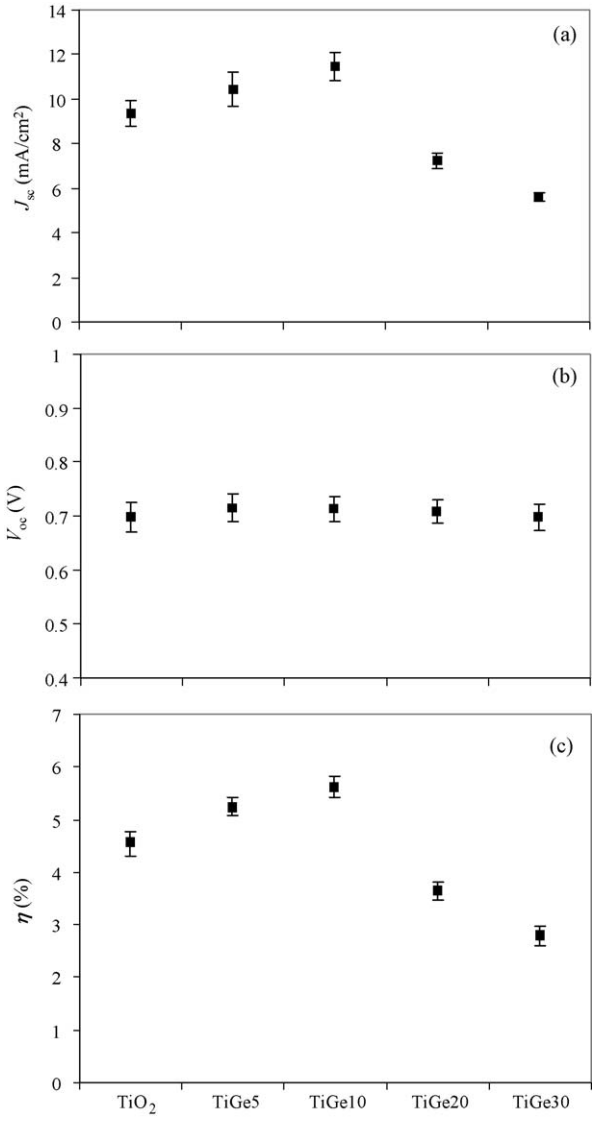

Fig. 4. Relation of photovoltaic characteristics and oxide composition. (a) Short-circuit current density (J_{sc}), (b) open-circuit voltage (V_{oc}) and (c) solar energy conversion efficiency (η).

was observed. This corresponds to the property of pure GeO_2 electrode. However, the results in Fig. 4b indicated that the addition of germanium (up to 30%) does not affect the V_{oc}.

Fig. 5 illustrates the dependence of J_{sc} on the thickness of the film prepared by the sample pure TiO_2 and TiGe10. It is clear that the J_{sc} obtained from TiGe10 electrode is higher than that obtained from pure TiO_2 electrode. The increasing of J_{sc} seems to get saturated with an increasing of thickness. Furthermore, when the thickness of TiGe10 film >7 μm, J_{sc} obtained from sample TiGe10 started to decrease. This is probably due to the fact that, the charge recombination between electrons injected from the excited dye to conduction band of semiconductor and the I_3^- ions in the electrolyte will become more serious in thicker films, which is detrimental to

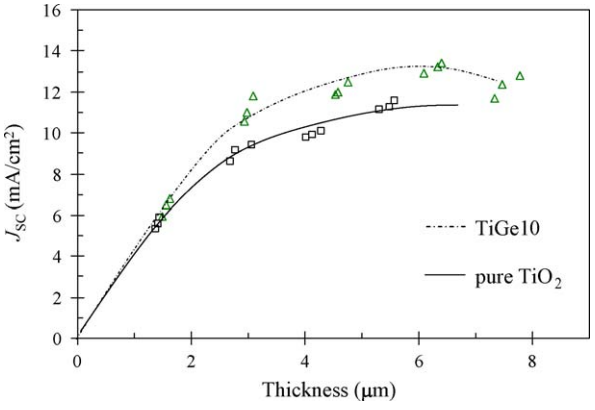

Fig. 5. Relationship between the short-circuit current density (J_{sc}) and thickness of electrodes fabricated by sample pure TiO_2 and TiGe10.

electron collection on the back contact, and thus, photocurrent generation [16]. In other words, the electrons generated at a distance farther from the interface between the electrode film and conducting glass are getting lost by recombination before they can reach the interface [2,17,18].

4. Conclusions

In summary, TiO_2, GeO_2 and binary TiO_2–GeO_2 oxides from different Ti/Ge ratio gels were synthesized by sol–gel method of surfactant-assisted mechanism. The XRD results indicated that these binary oxides were solid solutions because of the gradual shift of 1 0 1 diffraction peak of anatase type of TiO_2. The added germanium role was based on the crystal growth inhibiter, which leading to smaller grain size when compared to the sole metal oxide. The binary oxides samples had higher surface area than the pure component, which resulted in the higher amount of adsorbed dye concentration. The electrodes fabricated from sample TiGe5 and TiGe10 gave significant higher J_{sc} when compared to those of pure TiO_2. The use of binary oxide as an electrode was an alternative approach to enhance the efficiency of dye-sensitized solar cell.

Acknowledgements

This work was supported by a grant-in-aid from the Ministry of Education, Science Sports and Culture of Japan under the 21 COE program. The authors would like to express gratitude to Prof. Mochizuki at AIST for the kind supply of Pt counter electrode.

References

[1] M. Grätzel, Pure Appl. Chem. 73 (2001) 459–467.
[2] A. Kitiyanan, S. Ngamsinlapasathian, S. Pavasupree, S. Yoshikawa, J. Solid State Chem. 178 (2005) 1044–1048.
[3] A. Hagfeldt, M. Grätzel, Chem. Rev. 95 (1995) 49–68.
[4] L. Kavan, B. O'Regan, A. Kay, M. Grätzel, J. Electroanal. Chem. 346 (1993) 291–307.
[5] R. Dabestani, A.J. Bard, A. Campion, M.A. Fox, T.E. Mallouk, S.E. Webber, J.M. White, J. Phys. Chem. 92 (1988) 1872–1878.
[6] D.J. Fitzmaurice, H. Frei, Langmuir 7 (1991) 1129–1137.
[7] T.A. Heimer, S.T. D'Arcangelis, F. Farzad, J.M. Stipkala, G.J. Meyer, Inorg. Chem. 35 (1996) 5319–5324.
[8] F. Nuesch, J.E. Moser, V. Shklover, M. Grätzel, J. Am. Chem. Soc. 118 (1996) 5420–5431.
[9] H. Rensmo, K. Keis, H. Lindstrom, S. Sodergren, A. Solbrand, A. Hagfeldt, S.-E. Lindquist, L.N. Wang, M. Muhammed, J. Phys. Chem. B 101 (1997) 2598–2601.
[10] B. O'Regan, M. Grätzel, Nature 353 (1991) 737–739.
[11] L.M. Peter, K.G.U. Wijayantha, Electrochem. Commun. 1 (1999) 576–580.
[12] H. Rensmo, H. Lindström, S. Södergren, A.-K. Willstedt, A. Solbrand, A. Hagfeldt, S.-E. Lindquist, J. Electrochem. Soc. 143 (1996) 3173–3178.
[13] J.C. Yu, J. Lin, R.W.M. Kwok, J. Phys. Chem. B 102 (1998) 5094–5098.
[14] S. Ito, K. Ishikawa, C.-J. Wen, S. Yanagida, T. Watanabe, Bull. Chem. Soc. Jpn. 73 (2000) 2609–2614.
[15] Y. Saito, S. Kambe, T. Kitamura, Y. Wada, S. Yanagida, Sol. Energy Mater. Sol. Cells 73 (2004) 1–13.
[16] Z.-S. Wang, H. Kawakuchi, T. Kashima, H. Arakawa, Coord. Chem. Rev. 248 (2004) 1381–1389.
[17] K. Srikanth, Md.M. Rahman, H. Tanaka, K.M. Krishna, T. Soga, M.K. Mishra, T. Jimbo, M. Umeno, Sol. Energy Mater. Sol. Cells 65 (2001) 171–177.
[18] J. Jiu, F. Wang, M. Sakamoto, J. Takao, M. Adachi, J. Electrochem. Soc. 151 (2004) A1653–A1658.